Geofísica Internacional (2019) 58-1: 81-99

Original paper

Injection into the shallow aquifer-aquitard system beneath Mexico City for counteracting pore pressure declines due to deeper groundwater withdrawals: Analysis of one injection well

Felipe Vázquez-Guillén* and Gabriel Auvinet-Guichard

Received: April 24, 2018; accepted: September 20, 2018; published on line: January 18, 2019

Resumen

Los acuíferos están siendo severamente sobre-explotados en muchas partes del mundo conforme al continuo aumento de las poblaciones urbanas. Además, la excesiva extracción del agua subterránea de los acuíferos ha acelerado dramáticamente la consolidación de los acuitardos sobre-yacientes, creando severos hundimientos del terreno y muchos otros problemas relacionados. La Ciudad de México, con una población de 20 millones de habitantes y un acuífero principal exhausto, es un sitio que ofrece excelentes condiciones para experimentar técnicas de compensación. En este artículo, se propone una estrategia con el propósito específico de mitigar el hundimiento del subsuelo de la Ciudad de México. La estrategia consiste en aumentar la presión de poro en el acuífero somero por debajo de la Ciudad de México con la intención de inducir un proceso de difusión a través de los acuitados superior e inferior, para generar incrementos de presión de poro en el sistema que contrarresten los actuales descensos de presión de poro asociados a las extracciones de agua subterránea en la unidad acuífera principal. La estrategia se analiza analíticamente y se utilizan parámetros hidráulicos típicos del sistema acuífero-acuitado somero por debajo de la Ciudad de México sujeto a un pozo de inyección. Los resultados proporcionan, por primera vez, las respuestas hidráulicas acopladas del sistema sujeto a la inyección de agua y proporcionarán datos útiles cuando se realicen pruebas de inyección en el futuro cercano.

Palabras clave: Difusión inducida. Soluciones analíticas. Respuestas hidráulicas acopladas. Hundimiento del terreno.

Abstract

Aquifers are being severely overexploited in several sites around the world as urban populations continue to grow. Excessive groundwater subtraction of aquifers has also accelerated the consolidation of the overlying aquitards dramatically, creating severe land subsidence and many other related issues. Mexico City, with its population of 20 million inhabitants and depleted main aquifer, is a prime site for experimental approaches for redress. In this paper, a purpose-specific strategy for the land subsidence mitigation of Mexico City is suggested. The strategy consists of rising depleted pore pressure in the shallow aquifer beneath Mexico City to induce a diffusion process through the upper and lower aquitards that generate increments of pore pressure in the system to counteract current pore pressure declines associated to groundwater withdrawals of the main aquifer unit. The strategy is analyzed on the basis of analytical solutions and typical hydraulic parameters for the shallow aquifer-aquitard system beneath Mexico City subject to one injection well. The results provide for the first time the coupled hydraulic responses of the shallow aquifer-aquitard system beneath Mexico City subject to water injection and provides useful data for field injection tests to be conducted in the near future.

Key words: Induced diffusion. Analytical solutions. Coupled hydraulic responses. Land subsidence.

F. Vázquez-Guillén*
G. Auvinet-Guichard
Instituto de Ingeniería
Coordinación de Geotecnia
Universidad Nacional Autónoma de México
Ciudad Universitaria, Apdo. Postal 70-472
Coyoacán, 04510
CDMX, México.
Corresponding author: fvazquezg@exii.unam.mx

Introduction

Mexico City is located within the southwestern portion of the Basin of Mexico (Figure 1). Conventionally, the Valley of Mexico refers to the lowest area of this basin. It is essentially an extensive plain at an average altitude of 2240 m above sea level formed by low strength, very compressible, lacustrine clayey aquitards partially overlying highly productive regional aquifers of volcanic and sedimentary origin. Over 20 million people in Mexico City and its metropolitan area rely on groundwater as their main water resource. Currently, greater rates than can be naturally replenished are being subtracted from one of these aquifer units, so in several detected locations it is overexploited (Conagua, 2009; NRC, 1995).

Consequences of such excessive groundwater exploitation extend well beyond decreasing freshwater availability for residents in Mexico City. This exploitation has also accelerated the aquitard's consolidation dramatically, creating non-uniform spatially distributed land subsidence all over the Valley of Mexico. Areas where aquitards are at their thickest, subsidence may reach rates of 0.40 m per year (Auvinet *et al*., 2017). Zones where thickness and/or compressibility of aquitards vary steeply, differential settlements (from point-to-point) become so disparate that, beyond a certain limit, the soil begins to fracture (Auvinet *et al*., 2013). Soil fracturing has caused the collapse of buildings, breakage of water and sewage pipelines, wastewater flooding and leakages (Jimenez *et al*., 2004). Several studies have confirmed that through such fractures, aquifers are directly exposed to pollution caused by wastewater and garbage leaching (Mazari and Mackey 1993). In addition, large portions of the lacustrine sediments in the valley exhibit piezometric depressions (Figure 2a) and increments of effective stresses (grain-to-grain) (Figure 2b). As water exploitation continues, rates of subsidence and differential settlements increase constantly. This cumulative process makes both the size of the subsiding area and the damage on the built-up environment to increase. Under these conditions, building and/or maintaining the operational capacity of any engineered work within the valley requires prognoses of piezometric losses, rates of ground consolidation and subsoil deformations at the site in question (Reséndiz *et al*., 2016).

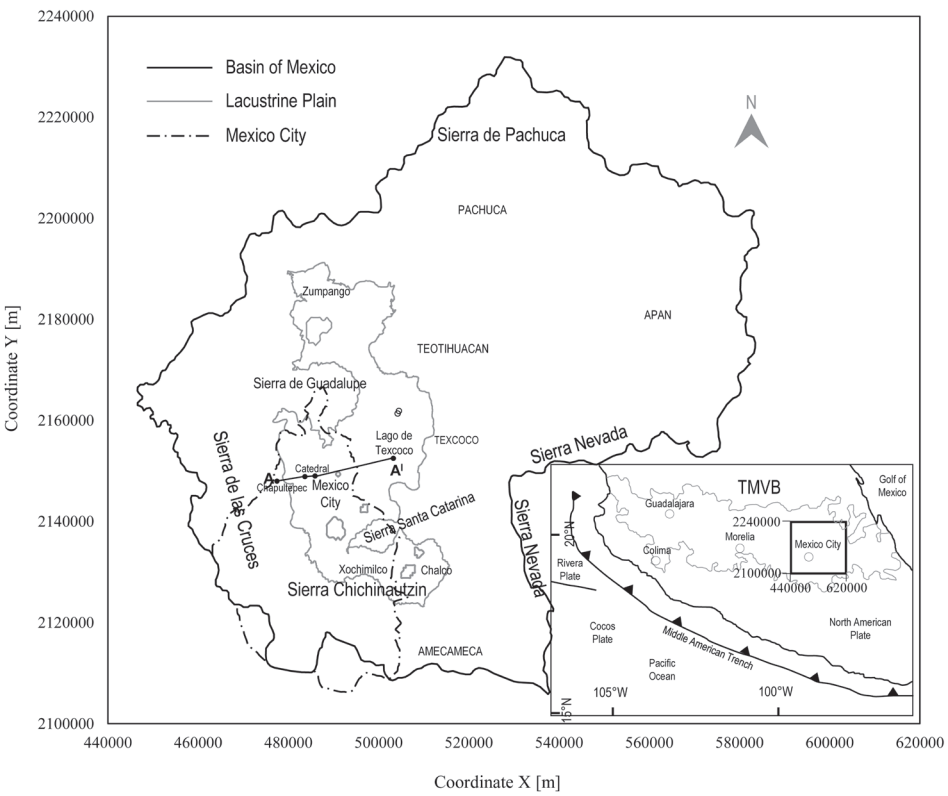

Figure 1. The location of Mexico City within the context of the Basin of Mexico. TMVB stands for Trans-Mexican Volcanic Belt.

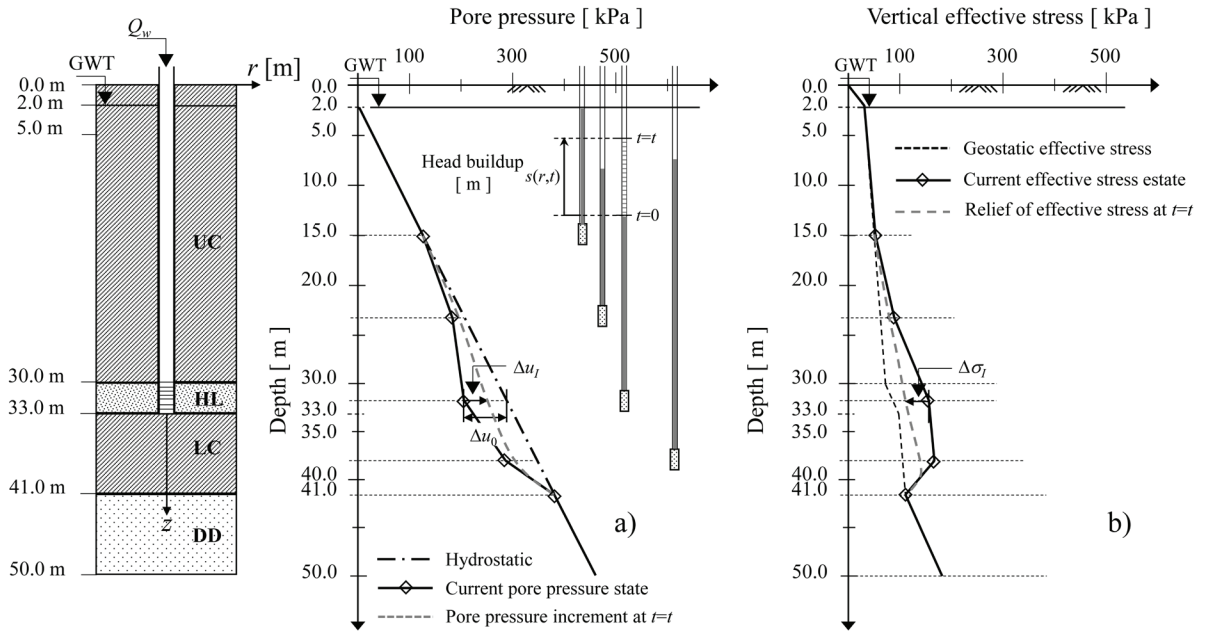

Figure 2. Profiles illustrating typical conditions in the lacustrine plain beneath Mexico City and the purpose of the injection well studied in our investigation: a) Pore pressure, b) Vertical effective stress. UC: Upper Clay; HL: Hard Layer; LC: Lower Clay; DD: Deep Deposits.

Over the last few decades, Comisión Nacional del Agua (Conagua) and Sistema de Aguas de la Ciudad de México (Sacmex) have implemented a program in Mexico City to deal with aquifer overdraft and meet the ever increasing water demand (Conagua, 2006; DGCOH, 1997; DGCOH and Lesser, 1991). Among the main actions of this program, one consists of artificially recharging the main production aquifer with treated waste water and/or rainfall water at a rate of 10 m^3/s using injection wells located to an average depth of ~150 m (DGCOH, 1997). Artificial recharge attempt to reduce the aquifer's overdraft within Mexico City's area estimated in ~22 m^3/s (World Bank, 2013). The authorities also expect to reduce land subsidence through this program, but this benefit is seen as a collateral effect; they are mostly concerned with restoring abstracted volumes of water to the main production aquifer safely.

The most significant efforts to implement a recharge program began at the end of the past century when water injection tests were conducted as part of the activities of "Proyecto Texcoco" (Cruickshank, 1998). This project aimed to create a storage wastewater reservoir consisting of several artificial lakes by consolidation of in-situ soils through groundwater extraction wells. Around the same time, aquifer recharge activities were implemented in other sites in Mexico City, specifically around the treatment plants in "Cerro de la Estrella" (19°20'11.58" N; 99° 4'29.21" O) and "San Luis Tlaxialtemalco" (19°15'29.87" N; 99° 1'46.31" O). Single-well injection rates of 0.05 m^3/s and of 0.06 m^3/s were used to recharge the main aquifer unit in these two sites (DGCOH, 1997). In 2007, as a result of these investigations, Conagua published the first official standards in the country regarding the recuperation of aquifers and protection of groundwater (NOM-014-Conagua-2007; NOM-015-Conagua-2007). Presently, the artificial recharge technique and the interaction between the native water and the injected water are still under examination (Huizar *et al*., 2016; Conagua, 2006).

Artificial recharge studies relating to Mexico City have examined the general performance of injection wells in the field (Cruickshank, 1998), the feasibility of using reclaimed wastewater as the injected water (Carrera and Gaskin, 2007; DGHOH, 1997), the impact of injecting treated wastewater on the quality of the native water (Conagua, 2006; DGHOH, 1997) and the rates at which water can be injected at specific sites (Cruickshank, 1998; DGCOH and Lesser, 1991). However, there has not been a study of underground injection for

land subsidence mitigation. Thus, this paper examines underground injection specifically as a strategy for the land subsidence mitigation of Mexico City. In other words, we investigated an injection well whose main purpose was not to restore abstracted volumes of water to the main aquifer unit, but rather, to counteract current pore pressure declines in the aquitards as a result of groundwater withdrawals. Figure 2 illustrates the setting of the injection well considered in our investigation. The results of this study provide for the first time the coupled hydraulic responses of the shallow aquifer-aquitard system beneath Mexico City subject to water injection and provides useful data for field injection tests to be conducted in the near future.

Principles of water injection into aquifer-aquitard systems

In alluvial, lacustrine and shallow-marine environments, clayey aquitards often appear interbedded and interfingered with sandy and gravelly aquifers. Aquifers may be confined and semiconfined by aquitards. Most of the times, there is a large permeability contrast between aquifers and aquitards and also aquitards are of a highly compressible nature. These characteristics make that an aquifer-aquitard system respond to fluid injection as a leaky-aquifer system for practical purposes. Leaky-aquifer systems are represented by alternating layers of aquifers and aquitards, each of which is characterized with its hydraulic conductivity, specific storage and thickness. Thus, the coupled hydraulic responses of leaky-systems (pore pressure responses, head buildup in aquifers and leakage rates through aquitards) involve the hydraulic parameters of both aquifers and aquitards. Several authors have discussed the hydrodynamics of wells in such systems (e.g. Neuman and Witherspoon, 1969; Herrera and Figueroa, 1969; Herrera, 1970; Herrera, 1976; Cheng and Morohunfola, 1993; Cihan *et al*., 2011). The theory of effective stress and one-dimensional consolidation (Terzaghi, 1925), is directly applicable to the understanding of the behavior of aquifer-aquitard systems subject to water injection (Domenico and Mifflin, 1965). Alternatively, the aquitard-drainage model can be used for the same purpose (Tolman and Poland, 1940).

In the following, a leaky-aquifer system consisting of one aquifer underlying one aquitard is considered. To better appreciate the impact of water injection on land subsidence mitigation, the phenomenon of land subsidence is explained first. Figure 3 illustrates a typical compressibility curve of Mexico City's clay that represents the consolidation of the overlying aquitard subject to the influence of groundwater withdrawals in the underlying aquifer. Due to the large permeability contrast between the aquifer and aquitard, head declines in the aquifer give rise to excess pore pressure in the aquitard that diminishes toward the land surface. A transient downward movement of water through the aquitard is thus induced that reaches a steady state condition when the hydraulic head in the aquitard equilibrates with the head change in the adjacent aquifer.

During the transient state condition, total stress in the aquifer-aquitard system remains constant, so changes in pore pressure are associated with equal and opposite changes in effective stress. As a result, effective stress (σ'_v) increases and a reloading of the aquitard takes place. Initially, the increment in effective stress in the aquitard may be small and thus, land subsidence may be so as well. However, as soon as the preconsolidation stress (σ'_p) is surpassed, the aquitard suffers deformations on the virgin loading curve with a sudden increase in compressibility and subsidence rate (stress path 1-2). This inelastic compression of the aquitard is responsible for the vast majority of land subsidence.

The injection well studied in our investigation attempts to counteract this ongoing process by increasing pore pressure in the aquitard by diffusion. As a result of this practice, the effective stress is decreased causing the aquitard to recover a small portion of the total deformation (stress path 2-3). Evidence of this response has been found during underground injection tasks conducted in several sites around the world (Zhang *et al*., 2015; Zhou and Burbey, 2014; Amelug *et al*., 1999), where decrements in effective stress have been indirectly verified by measuring expansions at specific hydro-stratigraphic units of the injection formation. For the shallow aquifer beneath Mexico City, the limiting value of the increment in pore pressure may be bounded by the hydrostatic profile, yet theoretically, only a small value is needed in order to mitigate subsidence. In practice, however, it is necessary that further increments of effective stress in the aquitard associated to groundwater subtraction of the main aquifer unit be counteracted by the injection well. After increments of effective stress in the aquitard have been counteracted, subsidence in Mexico City can be mitigated or even arrested. Otherwise, the tendency of subsidence will continue unabated (stress path 2-4).

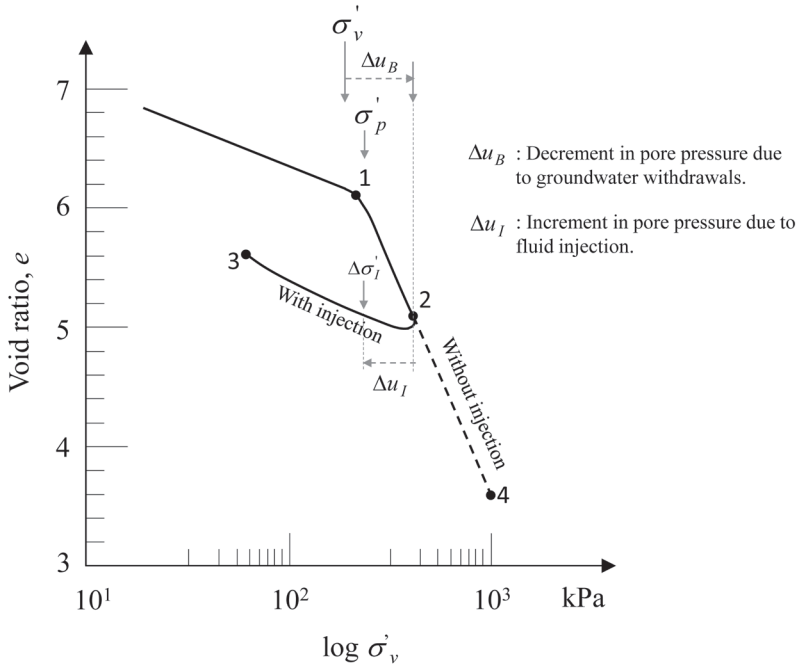

Figure 3. Typical compressibility curve of the Mexico City's clay illustrating the effects of groundwater extraction and water injection.

Previous applications of underground injection

The first applications of underground injection addressing land subsidence issues appeared within the oil industry. At the end of the 1950's, water injection into the subsurface was used to mitigate excessive surficial settlements originated by oil extraction in the Wilmington field, Long beach, California (Otott and Clarke, 1996). Later on, this strategy was adopted by several countries as a complementary policy for land subsidence mitigation and its implementation showed promising results (Poland, 1972; Poland, 1984). Cities where this practice has successfully been implemented include: Las Vegas (Amelug *et al*., 1999; Bell *et al*., 2008), Shanghai (Zhang *et al*., 2015; Shi *et al*., 2016) and Bangkok (Phien *et al*., 1998), among others. Depending on the magnitude of the induced expansions and the management of the groundwater extractions, land subsidence in these cities has been controlled, mitigated or arrested. Moreover, a water injection project led by the University of Padua which aims to uplift the city of Venice in order to protect it from periodic floods is at a very advanced stage of development (Gambolati and Teatini, 2014). Recently, the project has been studied carefully through numerical simulations (Teatini *et al*., 2010) and researchers expect to perform injection tests for calibrating the developed computational tools in the near future (Teatini *et al*., 2011). In Mexico City, however, injection sites have not been studied for their potential ability to mitigate land subsidence, despite several decades of injections for the purpose of water replenishment.

Shallow aquifer-aquitard system beneath Mexico City

The fill of the Mexico Basin comprises lacustrine and alluvial deposits. The upper most ~100-150 m of this fill has been described by several researchers (Marsal and Mazari, 1959; Zeevaert, 1982; Vázquez and Jaimes, 1989). For illustrative purposes, one stratigraphic cross-section E-W of the upper ~90 m of such fill is shown in Figure 4a. Specifically, the lacustrine deposits of the basin fill consist of low strength, highly compressible clays and allophanes (Ovando *et al*., 2013). The average thickness of the lacustrine deposits is ~40-50 m beneath Mexico City but increases significantly outside the city limits. Beneath Mexico City, lacustrine deposits are present in two formations –the upper and lower clay formations-- clearly divided by a lens of only a few meters thick composed mainly of sands, gravely sands, and thin lenses of soft silty clays (Ovando *et al*., 2013). The National Research Council called this permeable unit the "shallow aquifer" because it provided freshwater to

Mexico City in the mid to late 1800s (NRC, 1995). The soil mechanics community refers to this soil stratum as the first "hard layer" after Marsal and Mazari (1959). Overlying the upper clay formation, a crust of dried low plasticity silty clays is found, which in turn underlies an anthropogenic fill. The alluvial deposits of the basin fill, in contrast, comprise very consistent silts and sandy silts interbedded with hard clays. Marsal and Mazari (1959) refer to these soils as the "deep deposits" when they appear underlying the lower clay formation.

The vertical hydraulic conductivity of the aquitards varies between ~$5x10^{-9}$ ms^{-1} and ~$20x10^{-9}$ ms^{1}, whereas their specific storage coefficient is found in the range of ~$1x10^{-2}$ s^{-1} to ~$15x10^{-2}$ s^{-1} (Herrera *et al*., 1989). Marsal and Mazari (1959) demonstrated through geotechnical explorations that the clay sediments become stiffer and less permeable with depth. Some authors have found evidence of reduced hydraulic conductivity during field-permeability tests. Near the aquifer-aquitard interface, Rudolph *et al*. (1991) found values in the range of $2.5x10^{-9}$ ms^{-1} to ~$3.5x10^{-9}$ ms^{-1} in the Texcoco area, and Vargas and Ortega (2004) found values between $3x10^{-11}$ ms^{-1} and $3x10^{-10}$ ms^{-1} in one site near downtown Mexico City. For the hard layer, Rudolph *et al.* (1989) report average values of $1x10^{-4}$ ms^{1} and of $8x10^{-5}$ ms^{-1} for the hydraulic conductivity and values of $1x10^{-3}$ m^{-1} and of $2x10^{-3}$ m^{-1} for the specific storage coefficient. Herrera *et al.* (1989) report values for the horizontal hydraulic conductivity of the deep deposits generally ranging between $1x10^{-5}$ ms^{-1} and $15x10^{-5}$ ms^{-1} with isolated values of $0.01x10^{-5}$ ms^{-1} and values from $1x10^{-6}$ m^{-1} to $10x10^{-6}$ m^{-1} with isolated values of $0.01x10^{-6}$ m^{-1} for the specific storage coefficient.

Before extensive groundwater withdrawal from the shallow aquifer in the mid to late 1800s, both the regional aquifer and shallow aquifer were subject to artesian pressure (NRC, 1995), so natural discharge paths caused water to move upward through the aquitards (Durazo and Farvolden, 1989). Currently, extensive groundwater subtraction has inverted the gradients and water is now moving downward in most of this area (Ortega and Farvolden, 1989). Thus, aquitards are now contributing to the aquifer's yield by leakage flux which is derived mainly from a depletion of storage in the clayey aquitards.

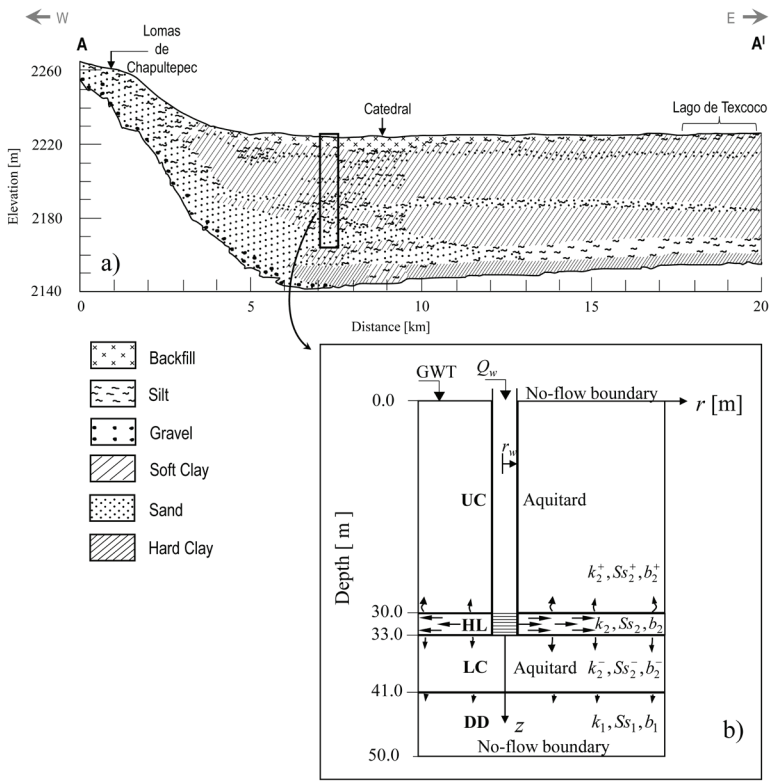

Figure 4. Illustration of the subsoil beneath Mexico City (Modified after Marsal and Mazari, 1959): a) Cross-section W-E through the lacustrine plain; the location of cross-section AA' is indicated in Figure 1, b) Conceptual model of the shallow aquifer-aquitard system.

On the basis of field and laboratory data collected over the last decades related to the compression of the upper aquitard in the central part of Mexico City (Ovando *et al*., 2003), it is estimated that leakage of the upper aquitard may account for ~50-60% of total land subsidence in this area. Leakage flux of aquitards together with the initial exploitation of the shallow aquifer may also explain the typical conditions for pore pressure decline observed in most of the lacustrine plain. Pore pressures in the upper ~15 m are often found at hydrostatic conditions, yet in deeper sandy layers within the clays, pore pressure depletion rates from 0.002 to 0.014 kPa per year have been reported by some research (Ovando *et al*., 2003). Hence, any injection project designed to mitigate aquitard's consolidation process induced by the depletion of pore pressures as a consequence of the exploitation of the main aquifer should increase pore pressure in aquitards to a faster rate. This paper provides a first estimate of pore pressure restoration rates taking into account the coupled flow in aquifers and aquitards on the basis of the following mathematical model.

Mathematical model for water injection

The mathematical model for water injection adopted here is based on a set of governing equations formulated to represent transient groundwater flow in a homogeneous and isotropic, confined multilayered aquifer-aquitard system of infinite horizontal extension with one injection well screened over the entire thickness of selected aquifers. Figure 4b illustrates one such system consisting of two aquifers and two aquitards. The flow pattern induced by the injection well is assumed to be horizontal in aquifers and vertical in aquitards. This assumption is widely used in practice as long as the hydraulic conductivity contrast between aquifers and adjacent aquitards is at least of one order of magnitude (Neuman and Witherspoon, 1969). The exchange of water that occurs through the aquifer-aquitard interfaces as a result of the injection of water is called leakage. In such leaky-systems, horizontal flow in aquifers is coupled with each other by accounting for diffuse leakage through aquitards according to the following system of governing equations.

Governing equations for multilayered systems

In terms of the hydraulic head buildup $s_i = s_i(r,\ t)$ [L], single-phase radial flow in aquifer i of the multilayered system is described by the following governing equation (Cihan *et al*., 2011):

$$\frac{1}{r}\frac{\partial}{\partial r}\left(r\frac{\partial s_i}{\partial r}\right)=\frac{1}{D_i}\frac{\partial s_i}{\partial t}+\frac{w_i^-}{T_i}+\frac{w_i^+}{T_i};\ i=1,\ldots,N, \tag{1a}$$

where $s_i = h_i(r,\ t)-h_{i0}$ with h_i [L] being the hydraulic head in aquifer i and h_{i0} the initial head in that aquifer. $D_i = k_i/Ss_i$ [L^2T^{-1}] is the hydraulic diffusivity where k_i [LT^{-1}] is the hydraulic conductivity and Ss_i [L^{-1}] is the specific storage coefficient of aquifer i. $T_i = k_i b_i$ [L^2T^{-1}] is the transmissivity with b_i [L] being the thickness of aquifer i. r [L] is the radial distance from the center of the well and t [T] is the time. w_i^α [LT^{-1}] denotes the rate of diffuse leakage (i.e. specific discharge) through the aquifer-aquitard interface from aquifer i into the overlying ($\alpha = +$) or underlying ($\alpha = -$) aquitard, and can be calculated according to:

$$w_i^\alpha = -\frac{k_i^\alpha}{b_i^\alpha}\frac{\partial s_i^\alpha}{\partial z_{D_i}^\alpha}\bigg|_{z_{D_i}^\alpha=0} \tag{1b}$$

where $s_i^a = s_i^a(r, z_{D_i}^a, t)$ [L] is the hydraulic head buildup in aquitard $(i,\ \alpha)$, k_i^a [LT^{-1}] is the hydraulic conductivity and b_i^a [L] is the thickness of that aquitard. $z_{D_i}^a = z_i^a / b_i^a$; $\{0 \le z_{D_i}^a \le 1\}$ is the dimensionless local vertical coordinate and z_i^a [L] is the local vertical coordinate, with $z_i^a = 0$ at the interface between aquifer i and aquitard $(i,\ \alpha)$, and $z_i^a = b_i^a$ at the interface between aquifer $i+\alpha$ and aquitard $(i,\ \alpha)$. Note that $i+\alpha = i+1$ for $\alpha = +$, while $i+\alpha = i-1$ for $\alpha = -$.

The vertical flow through aquitard $(i,\ \alpha)$ is described by the well-known diffusion equation:

$$\frac{\partial^2 s_i^\alpha}{\partial z_{D_i}^{\alpha\ 2}}=\frac{(b_i^\alpha)^2}{D_i^\alpha}\frac{\partial s_i^\alpha}{\partial t};\ 0 \le z_{D_i}^\alpha \le 1 \tag{2a}$$

subject to boundary conditions at aquifer-aquitard interfaces:

$$\begin{aligned} s_i^\alpha(r,0,t) &= s_i(r,t) \\ s_i^\alpha(r,1,t) &= s_{i+\alpha}(r,t), \end{aligned} \tag{2b}$$

where $D_i^\alpha = k_i^\alpha / Ss_i^\alpha$ is the hydraulic diffusivity and Ss_i^α is the specific storage coefficient of aquitard $(i,\ \alpha)$. In equation (2b), there is a relationship such that $s_i^+(r, z_{D_i}^+, t) = s_{i+1}^-(r, z_{D_{i+1}}^-, t)$ for $z_{D_{i+1}}^- = 1 - z_{D_i}^+$.

Assuming that the entire system of aquifers and aquitards is at hydrostatic pressure at $t = 0$, the initial conditions for the system can be written as:

$$s_i(r, t=0) = 0, \quad s_i^{\alpha}(r, z_{D_i}^{\alpha}, t=0) = 0. \tag{3}$$

Outer boundary conditions are:

$$s_i(\infty, t) = 0, \quad s_i^{\alpha}(\infty, z_{D_i}^{\alpha}, t) = 0. \tag{4}$$

The top and bottom boundaries of the system may have either a zero head buildup or a non-flow condition:

$$s_1^{-}(r,1,t) = 0 \text{ or} \tag{5a}$$

$$\partial s_1^{-}(r,1,t) / \partial z_{D_1}^{-} = 0, \tag{5b}$$

$$s_N^{+}(r,1,t) = 0 \text{ or} \tag{6a}$$

$$\partial s_N^{+}(r,1,t) / \partial z_{D_N}^{+} = 0. \tag{5a}$$

As mentioned above, Equations (1)-(6) couple the one-dimensional radial flow in aquifers with each other through the vertical flow in aquitards.

Boundary conditions for one injection well

In presence of one injection well with constant or time-dependent injection rate, the boundary condition at the radial wall of the cylindrical well interval screened in any aquifer is written as:

$$-2\pi r_{wi} T_i \frac{\partial s_i(r_{wi}, t)}{\partial r} = Q_i(t); \; i = 1, \ldots, N, \tag{7}$$

where $Q_i(t)$ is the injection rate through the injection well with radius r_{wi} fully screened into aquifer i, and s_i is the corresponding head buildup in that aquifer. Conventionally, $Q_i(t) > 0$ is used for injection. As a first approximation, no skin effect nor well bore storage are taken into account.

Analytical solutions for one injection well

Analytical solutions to Equations (1)-(7) were obtained by Cihan *et al*. (2011a,b) using the Laplace transform method. The solution procedure essentially consists of transforming the governing equations into the Laplace-domain (Cihan *et al*., 2011a; Cheng and Morohunfola, 1993; Zhou *et al*., 2009) and solving the resulting system of ordinary differential equations by applying the eigenvalue analysis method (Churchill, 1966; Hunt, 1985). The set of analytical solutions used in this paper are explained in the sequel.

The head buildup in the aquifers of a multilayered system with one injection well and diffuse leakage is given by:

$$\tilde{s}_i = \sum_{j=1}^{N} c_j^I \xi_{i,j} K_0\left(r\sqrt{\lambda_j}\right), \text{ or} \tag{8a}$$

$$c_j^I = 1 \Big/ \left(2\pi E_{i,j}^I\right) \sum_{k=1}^{N} \tilde{Q}_k(p) \xi_{k,j}, \tag{8b}$$

where c_j^I are the coefficients obtained from the boundary condition at the injection wellbore which are expressed as a function of the Laplace variable p (representative of time), $\tilde{Q}(p)$ is the Laplace transform of Equation (7) (Cihan *et al*., 2011), K_0 is the zeroth-order modified Bessel function of second kind, $E_{i,j}^I = r_{wi}\sqrt{\lambda_j} K_1(r_{wi}\sqrt{\lambda_j})$ with $E_{i,j}^I = 1$ as $r_{wi} \to 0$, where K_1 is the first-order modified Bessel function of second king. λ and ξ are the eigenvalues and eigenvectors, respectively, of the eigenvalue system $(\mathrm{A}' - \lambda \mathrm{I})\xi' = 0$ with $\mathbf{A}' = \mathbf{T}^{1/2}\mathbf{A}\mathbf{T}^{-1/2}$ and $\xi' = \mathrm{T}^{1/2}\xi$, where $\mathbf{A}$ is a matrix of dimension N x N referred to as the diffuse-leakage-coupling matrix, $\mathbf{T}$ is the diagonal transmissivity matrix of dimension N x N with components T_i and $\mathbf{I}$ is a unit diagonal matrix.

The rate of diffuse leakage through the aquifer–aquitard interface between aquifer i and its neighboring aquitard (i, α) can be calculated by integration of the diffuse leakage over the entire interface area (Zhou *et al*., 2009):

$$\tilde{Q}_i^{\alpha} = 2\pi \int_0^{\infty} \tilde{w}_i^{\alpha}(r,p) r dr = \sum_{j=1}^{N} \sum_{k=1}^{N} \frac{\left(f_i^{\alpha}\xi_{i,j} - g_i^{\alpha}\xi_{i+\alpha,j}\right)}{\lambda_j} \xi_{k,j} \tilde{Q}_k(p); \quad i = 1, \ldots, N. \tag{9}$$

where $\tilde{w}_i^{\alpha}(r,p) = f_i^{\alpha}\tilde{s}_i - g_i^{\alpha}\tilde{s}_{i+\alpha}$ is the Laplace transform of the diffuse leakage. f_i^{α} and

g_i^{α} are functions that depend on the type of boundary conditions specified at the top and bottom boundaries of the system.

For the particular case of a multilayered system with no-flow condition specified at the bottom boundary (Equation 5b) or at the top boundary (Equation 6b), the corresponding equations for the head buildup in aquitards become:

$$\tilde{s}_i^{\alpha} = \left(r, z_{D_i}^{\alpha}, p\right) = \tilde{s}_i \frac{\cosh\left[\kappa_i^{\alpha}\left(1 - z_{D_i}^{\alpha}\right)\right]}{\cosh(\kappa_i^{\alpha})}, \quad (10a)$$

with:

$$\kappa_i^{\alpha}\left(p\right) = \sqrt{p/D_i^{\alpha}}\, b_i^{\alpha}, \quad (10b)$$

and the functions f_i^{α} and g_i^{α} are given by:

$$f_i^{\alpha}\left(p\right) = \left(\kappa_i^{\alpha}/b_i^{\alpha}\right)\kappa_i^{\alpha} \tanh\left(\kappa_i^{\alpha}\right), \quad (11a)$$

$$g_i^{\alpha}\left(p\right) = 0. \quad (11b)$$

Solutions to Equations (8)-(11) are obtained here using the computational code ASLMA (Cihan *et al*., 2011b). Details of the analytical solution procedure and its verification process can be found elsewhere (Cihan *et al*., 2011a; Cheng and Morohunfola, 1993). Analytical solutions calculate the transient behavior of pressure buildup in aquifers and aquitards and the rate of diffuse leakage through aquitards.

Conceptual model and its hydraulic characterization

In the present analysis, one cross-section that is deemed to be representative of the shallow aquifer beneath Mexico City is considered (Figure 4a). Then, it is simplified to a multilayered aquifer-aquitard system which consists of two-aquifers and two aquitards (Figure 4b). The aquifer between aquitards represents the shallow aquifer, whereas the overlying and underlying aquitards characterize the upper and lower clay formations. The lower aquifer represents the deep deposits. An injection well with a radius of 0.15 m is drilled vertically through the upper three layers. Then, the injection well is cased throughout the upper two layers, but it is screened over the entire thickness of the intermediate aquifer, which is the shallow aquifer. Layers of the system are assumed to be horizontal. A confined system whose lateral boundaries extend to infinity is assumed. Thus, the ground surface and bottom of the model are no-flow boundaries. The system is assumed to be under hydrostatic equilibrium with respect to the hydraulic head. Hence, computed pore pressures are in fact values in excess of the hydrostatic profile and the effect of a non-hydrostatic initial equilibrium on the relative increments in pore pressure with depth is assumed to be negligible. The conditions under which the analysis is conducted are also assumed to be representative of one injection well outside the influence range of any pumping well into the deeper production aquifer. For this analysis, hydraulic properties typical of the shallow aquifer-aquitard system beneath Mexico City area are chosen (Table 1). Values of specific storage for the upper and lower clay formations used in the analysis consider the less compressible character of the soils under the unloading stress paths imposed by the injection well, in agreement with the recommendations of several authors (Marsal and Mazari, 1959; Teatini *et al*., 2010; Teatini *et al*., 2011; Gambolati and Teatini, 2014).

Table 1. Hydraulic properties used in the conceptual model of the shallow aquifer-aquitard system beneath Mexico City subject to one injection well. UC: Upper Clay; HL: Hard Layer; LC: Lower Clay; DD: Deep Deposits.

Unit	Material	b [m]	k [ms^{-1}]	T [m^{2}s^{-1}]	Ss [m^{-1}]	S [--]
UC	Very soft and highly compressible clay.	30.0	5.0x10-9	1.5x10-7	0.015	0.45
HL	Very dense clayey sand.	3.0	5.0x10-5	1.5x10-4	1x10-4	0.0003
LC	Soft and highly compressible clay.	8.0	1.0x10-9	8.0x10-9	0.005	0.04
DD	Very dense silty sand and gravel.	9.0	1x10-4	9.0x10-4	5x10-5	0.00045

Computed hydraulic responses and discussion

Coupled hydraulic responses as a function of time of the shallow aquifer-aquitard system beneath Mexico City subject to water injection are analyzed in this section. Injection rates of 0.002 m^3s^{-1} and of 0.004 m^3s^{-1} and injection periods of 1000 d and of 5000 d are considered for analyzing the hydraulic responses. The analyzed responses comprise pore pressure responses in the entire system, head buildup in aquifers and leakage rates through aquitards. The assessment of leakage rates through the aquitards is necessary to quantify the amount of water that is transferred from the injection aquifer to adjacent aquifers through the aquitards.

Pore pressure responses

Plots of Figure 5 show the effect of the injection rate on pore pressure development at the contact between the injection aquifer (HL) and the upper clay (UC) formation. Pore pressure is plotted as a function of the radial distance from the injection well center for two injection periods. The results shown in Figure 5a and Figure 5b correspond to injection rates of 0.004 m^3s^{-1} and 0.002 m^3s^{-1}, respectively. From both plots, it is observed that pore pressure decreases as injection rate decreases and dissipates very fast near the injection well. Away from 15 m of the injection well center, pore pressure reduction becomes more gradual. The dashed line plotted in both figures indicates an upper threshold for pore pressure development calculated as the sum of the vertical effective stress at the bottom of the UC formation and the undrained shear strength of this formation at that depth. Assuming an average undrained resistance for the UC formation equal to 70 kPa at 30 m depth on the basis of the values reported by Marsal and Mazari (1959) and reading from Figure 2b a typical value for the effective vertical stress equal to 140 kPa at that depth, the upper threshold for pore pressure development yields 210 kPa. This is an estimated upper limit that should not be exceeded in order to avoid hydraulic fracturing of the UC at the contact with the HL. As can be observed in Figure 5a, an injection rate of 0.004 m^3s^{-1} induces pore pressure slightly higher than such limit very near the injection well and therefore this rate may not be adequate in some practical situations. However, the numerical value for avoiding the hydraulic fracturing of the clay may vary from site to site, and therefore it should be accurately determined in all cases.

The effect of the injection period can also be seen in the plots of Figure 5. It shows that in passing from 1000 d to 5000 d of injection, pore pressure does not increase significantly near the injection well. As the distance increases, pore pressure is increased around 15-20 kPa for an injection rate of 0.004 m^3s^{-1} (Figure 5a) and around 10 kPa for an injection rate of 0.002 m^3s^{-1} (Figure 5b).

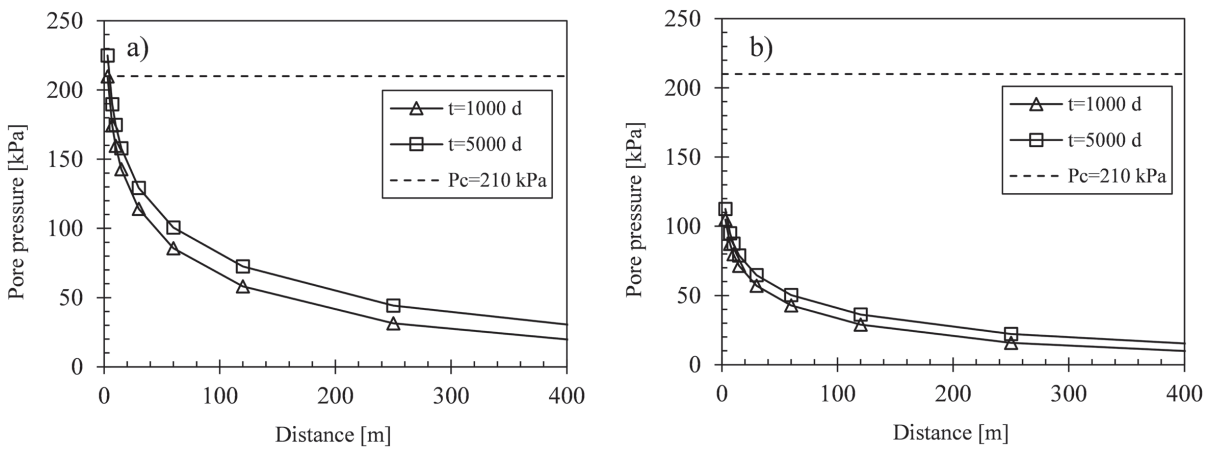

Figure 5. Effect of the injection rate and injection period on pore pressure development at the interface between the injection aquifer and the upper clay formation: a) The injection rate is Q_w=0.004 m^3s^{-1}, b) The injection rate is Q_w=0.002 m^3s^{-1}. Pc is an estimated upper threshold for pore pressure development below which hydraulic fracturing of the UC is avoided.

In order to evaluate the impact of the transmissivity of the injected formation on pore pressure development, two additional cases are now considered. The results of these analyses are shown in the plots of Figure 6. In the first case (Figure 6a), the transmissivity of the injection aquifer is increased by one order of magnitude and in the second case (Figure 6b) the transmissivity is decreased by one order of magnitude. Again, the dashed line in both plots represents the estimated upper limit for pore pressure development. It can be observed from Figure 6a that as the transmissivity of the injection aquifer increases, a higher rate of water can be injected into the aquifer without inducing pore pressure beyond the limit for hydraulic fracturing of the clay. The injection rate may even be as high as 0.03 m^3s^{-1}. However, Figure 6b indicates that as transmissivity of the injection aquifer decreases, it is necessary to reduce the injection rate dramatically in order to avoid hydraulic fracturing. In this last case, the injection rate may be as low as 0.00045 m^3s^{-1}. Therefore, the transmissivity of the injection aquifer is one of the variables with higher impact in the water injection task and this parameter should be accurately determined in the field. This finding is consistent with the results of stochastic simulations of multiphase flow. The importance of the permeability of the injection formation in application to geological CO_2 storage was pointed out in González *et al*. (2015). Authors found that the aquifer permeability have a significant influence on the pore pressure producing a wide-spread range of fluid overpressure in their stochastic analysis. As explained above, the injection period does not increase pore pressure significantly, especially near the injection well, even though the injection period increases from 1000 d to 5000 d.

Pore pressure fields through the aquifer-aquitard system generated by the injection well are shown in Figure 7 and Figure 8. The pore pressure fields of Figures 7a and 7b correspond to an injection rate of 0.002 m^3s^{-1} and injection periods of 1000 d and 5000 d, respectively. Figures 8a and 8b show pore pressure fields corresponding to an injection rate of 0.004 m^3s^{-1} and injection periods of 1000 d and 5000 d, respectively.

For both injection rates and injection periods, the highest increments in pore pressure are observed very near the injection well, at the interface between the HL and the UC and LC formations. As the injection period increases, pore pressure propagates longer distances in both directions of the Cartesian plane. Namely, for an injection rate of 0.002 m^3s^{-1}, pore pressure increments are observed at a depth of ~10 m after 1000 d of injection very near the injection well, but when the injection period increases to 5000 d, pore pressure increments extend vertically upward from the injection aquifer significantly. In the horizontal direction, pore pressure increments are observed 800 m away from the injection well center for an injection period of 1000 d and beyond 1000 m for 5000 d of injection. For an injection rate of 0.004 m^3s^{-1} and an injection

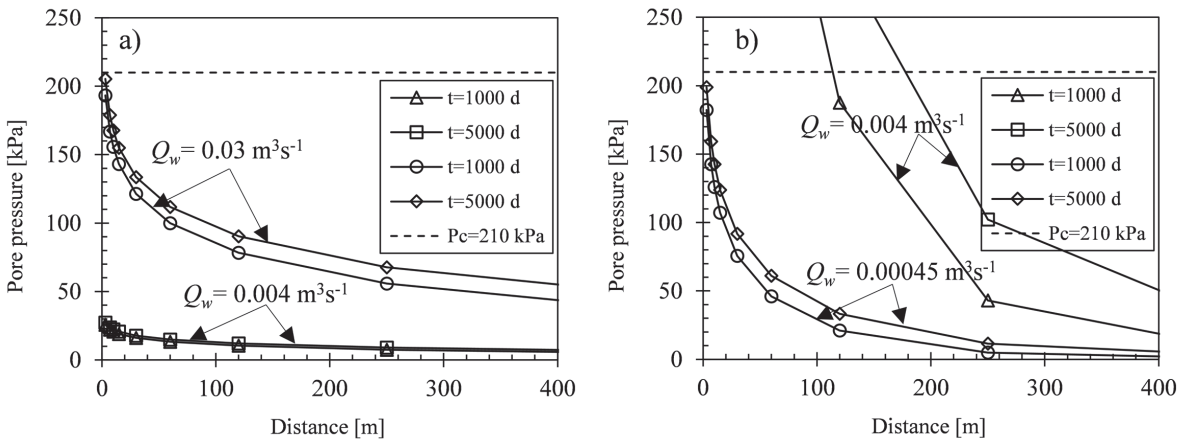

Figure 6. Effect of transmissivity of the injection aquifer on pore pressure development at the interface between the injection aquifer and the UC formation: a) The transmissivity of the injection aquifer is 1.5 x 10^{-3} m^2s^{-1}, b) The transmissivity of the injection aquifer is 1.5 x 10^{-5} m^2s^{-1}.

period of 5000 d, pore pressure propagates vertically upward until it reaches a depth of ~0.25 m near the injection well. According to results in Figure 5a, however, there is a risk of hydraulic fracturing of the UC formation very near the injection well for such an injection rate. Considering the significant benefit of injecting rates of the order of 0.004m^{3}s^{-1}, we suggest that investing sufficient resources is warranted to accurately determine the threshold at which hydraulic fracturing of the clay can occur during underground injection tasks.

Table 2 summarizes increments of pore pressure in the aquifer-aquitard system as a function of the radial distance from the injection well center, depth from the surface and injection rate after 1000 d of injection (see Figure 2a for explanation of the variables). The percentages reported in the table are calculated as the ratio of the increment in pore pressure generated by the injection well and the initial decrement in pore pressure, which is calculated as the difference between the actual and the hydrostatic profiles at corresponding

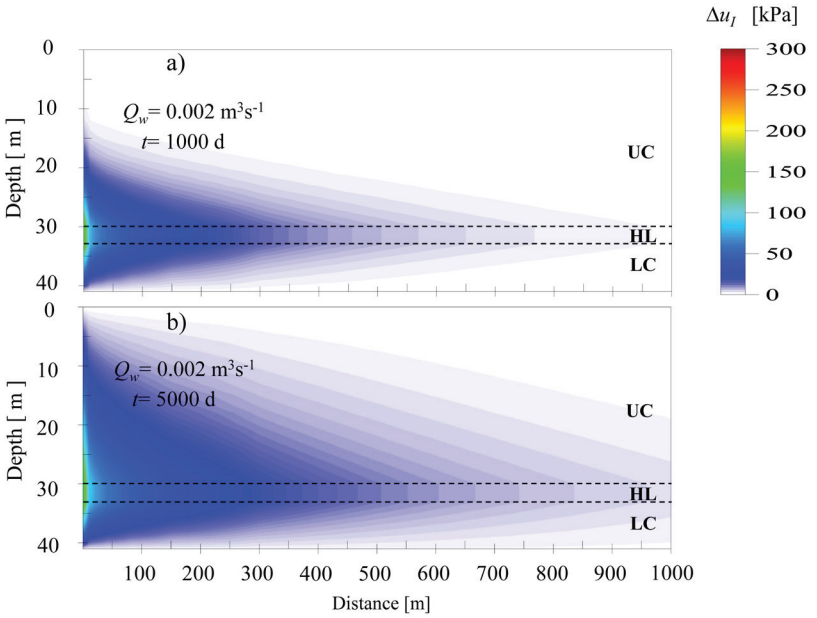

Figure 7. Pore pressure fields for an injection rate equal to 0.002 m^{3}s^{-1}: a) After 1000 d of injection, b) After 5000 d of injection.

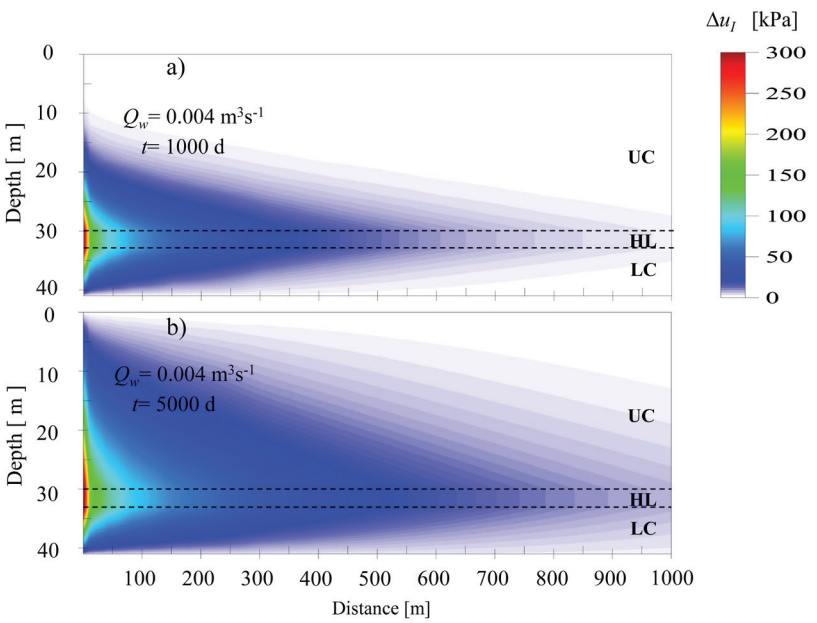

Figure 8. Pore pressure fields for an injection rate equal to 0.004 m^{3}s^{-1}: a) After 1000 d of injection, b) After 5000 d of injection.

depths (Figure 2a). The results reported in Table 2 indicate that for an injection rate of 0.002 m^3s^{-1}, ~19% of the initial deficit in pore pressure is restituted in UC formation at a depth of 23.5 m and 250 m away from the injection well center. At a depth of 38 m, ~7% of the initial deficit in pore pressure is restituted in the LC formation at 250 m away from the injection well. Note also that for the same injection rate, pore pressure in the Hard Layer (HL) does not exceed the hydrostatic conditions since only ~25.8% of the initial deficit in pore pressure is restituted in that formation. As the radial distance from the injection well increases, such values become smaller. Note, too, that pore pressure can be raised safely by maintaining the same injection rate of 0.002 m^3s^{-1}, but increasing the injection period. The corresponding values achieved by injecting a higher amount of water into the HL, for instance 0.004 m^3s^{-1}, indicates more appealing results, yet such injection rates should not be considered in pore pressure restitution projects within the lacustrine semiconfined aquifer of Mexico City unless the integrity of the UC formation can be confirmed.

Computed pore pressure restoration rates (r_u) as a function of the injection rate for different depths and radial distances from the injection well center are reported in Table 3. For an injection rate of 0.002 m^3s^{-1}, pore pressure in the UC formation (23.5 m depth) increases at a rate of 1.82-0.22 kPa per year, whereas in the LC formation (38.0 m depth), pore pressure increases at a rate of 1.64-0.23 kPa per year. Higher pore pressure restoration rates are found in the injection formation, as expected, and also when the injection rate increases. The reported restoration rates are significantly higher than the pore pressure depletion rates measured in the field by some researchers (Ovando *et al*., 2003). However, it should be noted that the present analysis is conducted in the absence of any pumping well into the deeper production aquifer. Thus, lower pore pressure restoration rates than those reported here may be expected in the field. This is particularly true in the area of the shallow aquifer-aquitard system that remains confined, which according to Carrera and Gaskin (2007) is located toward the central part of the lacustrine plain.

Table 2. Percentages of pore pressure restituted in the aquifer-aquitard system after 1000 d of injection.

					r=250 m		r=500 m		r=750 m	
Q_w [m^3s^{-1}]	Unit	z [m]	u_0 [kPa]	Δu_0 [kPa]	Δu_l [kPa]	$\Delta u_l/\Delta u_0$ [%]	Δu_l [kPa]	$\Delta u_l/\Delta u_0$ [%]	Δu_l [kPa]	$\Delta u_l/\Delta u_0$ [%]
0.002	UC	23.5	182.8	26.4	4.99	18.90	1.66	6.29	0.60	2.27
	HL	31.5	224.8	60.8	15.69	25.80	6.00	9.87	2.48	4.08
	LC	38.0	282.4	62.4	4.48	7.18	1.58	2.53	0.62	0.99
0.004	UC	23.5	182.8	26.4	9.97	37.76	3.33	12.61	1.20	4.54
	HL	31.5	224.8	60.8	31.38	51.61	12.02	19.77	4.96	8.16
	LC	38.0	282.4	62.4	8.96	14.36	3.16	5.06	1.24	1.99

Table 3. Computed pore pressure restoration rates.

			r=250 m	r=500 m	r=750 m
Q_w [m^3s^{-1}]	*Unit*	z [m]	r_u [kPa/year]	r_u [kPa/year]	r_u [kPa/year]
0.002	UC	23.5	1.82	0.61	0.22
	HL	31.5	5.73	2.19	0.91
	LC	38.0	1.64	0.58	0.23
0.004	UC	23.5	3.64	1.21	0.44
	HL	31.5	11.45	4.39	1.81
	LC	38.0	3.27	1.15	0.45

Head buildup in aquifers

Head buildup in aquifers at a distance of 15 m from the injection well center is plotted in Figure 9 as a function of time for an injection rate of 0.004 m^3s^{-1}. As expected, higher head buildup is induced in the injection aquifer (HL, triangles) than in the deep deposits (DD, diamonds). A steady state condition in the injection aquifer is not reached before 10000 d of injection. Thus, a steady state flow condition through the hard layer is not as easily reached as some authors (e.g. Zeevaert, 1982) indicate. After 100 d of injection, head buildup starts developing in the DD (diamonds), but the increments are very small. After 10000 d of injection, the head buildup is lower than 1 m. Therefore, for injection periods shorter than 10000 d, it seems sufficient to measure head buildup in the injection aquifer only during underground injection tasks, since negligible changes in head buildup within the DD should be expected.

Leakage rates through aquitards

Figure 10 plots leakage rates crossing the bottom (squares) and top (triangles) boundaries of the HL as a function of time for an injection rate of 0.004 m^3s^{-1}. From a short period of time after the beginning of injection to 1000 d, the rate of water crossing both boundaries increases. Higher leakage rates cross the top boundary of the injection aquifer during this period of time because the UC formation is more permeable. After 1000 d of injection leakage rates that cross the upper boundary increase and leakage rates that cross the lower boundary decrease because the UC formation has greater storage capacity. Note that such decrement in leakage rates is associated with a decrement in the leakage rates within the DD (Figure 11) because of flow continuity. As the injection period becomes longer, comparatively large amounts of water seep through the UC formation. Leakage rates crossing the bottom boundary of the injection aquifer are lower than 0.001 m^3s^{-1} even for long injection periods.

Figure 11 presents the behavior of leakage rates crossing the top boundary of the DD as a function of time. Again, the injection rate is equal to 0.004 m^3s^{-1}. A quite short period of time (100 d) is needed for the injection of the HL to influence the DD because the thickness of the LC formation is quite small (only 8 m). From 100 d to 1000 d of injection, leakage rates increase. However, a rather small leakage rate (lower than 0.000008 m^3s^{-1}), reaches the DD after 1000 d of injection. As the injection period increases, this leakage rate tends to a very small value. This is in agreement with Figure 9 for DD results. At time t=10000 d, head buildup seems constant. Note that the decrement in leakage rates for longer periods of time corresponds to the steady state condition that is reached in the UC formation, as the leakage rate in the upper aquitard tends to the injection rate value. Considering the leakage rate crossing the LC formation, an insignificant influence is expected of the injected water on the physical-chemistry composition of the native water in the DD, provided the injected and native water are compatible in quality.

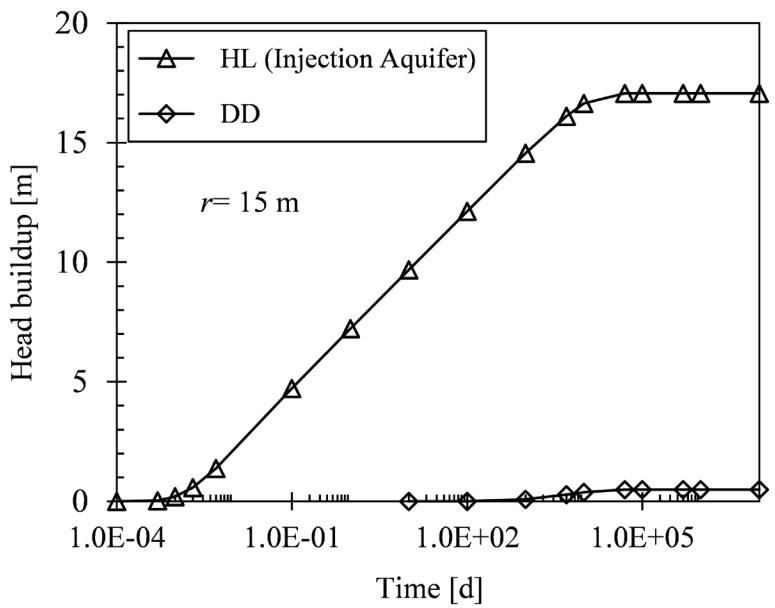

Figure 9. Estimated head buildup versus time for the injection aquifer (HL) and the Deep Deposits (DD).

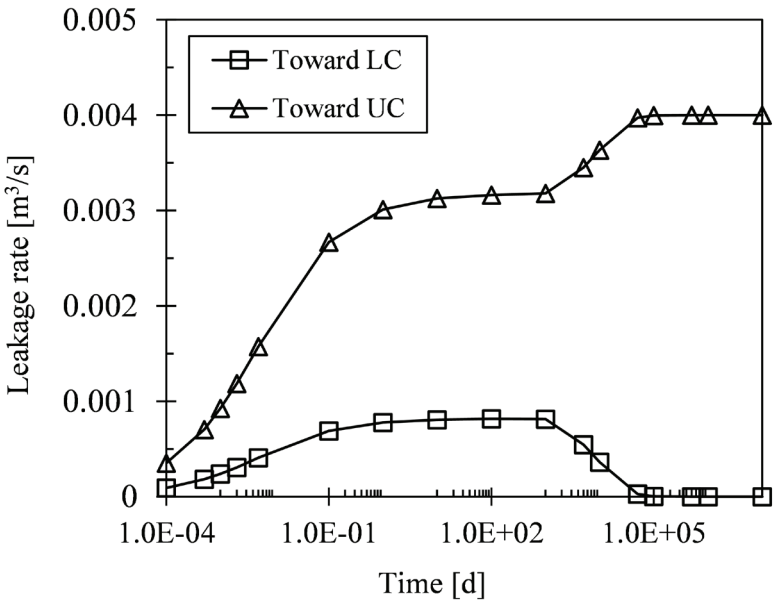

Figure 10. Leakage rates crossing the bottom (squares) and top (triangles) boundaries of the injection aquifer as a function of time.

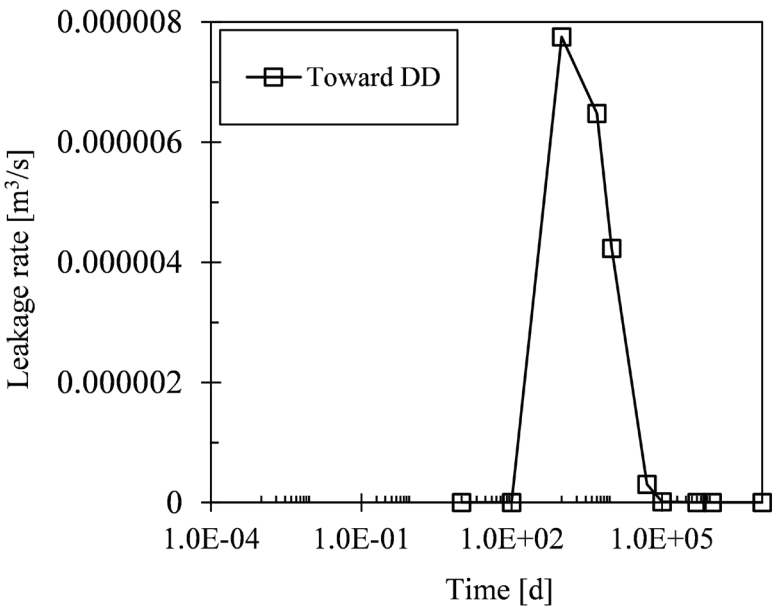

Figure 11. Leakage rates crossing the top boundary of the deep deposits (DD) as a function of time.

Conclusions

In this paper, a purpose-specific strategy for the land subsidence mitigation of Mexico City was suggested. This strategy consists of rising depleted pore pressure in the shallow aquifer beneath Mexico City to induce a diffusion process through the upper and lower aquitards. This diffusion process then generates increments of pore pressure in the system to counteract current pore pressure declines associated to groundwater withdrawals from the main aquifer unit. The analysis of this strategy was conducted under transient flow conditions on the basis of analytical solutions and typical hydraulic parameters for the shallow aquifer-aquitard system beneath Mexico City subject to one injection well. The results of the analysis comprise pore pressure responses in the entire system, head buildup in aquifers and leakage rates through aquitards. The main results of this analysis can be summarized as follows:

1. The transmissivity of the injection formation dominates the amount of pore pressure that is generated at the interface

between the injection aquifer and the upper and lower clay formations near the injection well center.

2. For a give transmissivity of the injection aquifer, injection rate and injection period determine the distance at which pore pressure is propagated through the system. The greater the injection rate and the longer the injection period, the longer the distances pore pressure is propagated through the system in both directions. Considering average values for the hydraulic parameters of the shallow aquifer-aquitard system beneath Mexico City and an injection rate of 0.002 m^3s^{-1}, pore pressure increments are observed 800 m away from the injection well center after 1000 d of injection and well beyond 1000 m after 5000 d of injection.

3. Computed pore pressure restoration rates are significantly higher than the pore pressure depletion rates measured in the field by some research (Ovando *et al*., 2003). Our results are representative of one injection well outside the influence range of any pumping well into the deeper production aquifer.

4. The injection into the shallow aquifer has a minor influence on the head buildup of the deep deposits. After 10000 d of injection, head buildup is lower than 1 m. Furthermore, contrary to some authors' suggestions (Zeevaert, 1982), a steady state condition in the injection aquifer is not easily reached in the short-term. This may take more than 10000 d of injection.

5. The amount of water that is transferred from the injection aquifer to the deep deposits through the lower clay formation is very small. As the injection period increases, this rate tends to zero because the leakage rate in the upper clay formation tends to the injection rate value. Thus, most of the injected water is transferred to the upper clay formation as the injection period increases.

The strategy for land subsidence mitigation advanced here is strongly based on well-established theoretical principles and has been implemented in several cities around the world with success. The benefits of controlling land subsidence in Mexico City are so immense that our strategy is worthy of further exploration. A first estimate of its benefits was provided here. Furthermore, the results reported in this paper are central in designing a field injection test into the shallow aquifer-aquitard system beneath Mexico City. However, it is recognized that in practice the hydraulic responses of the system may be influenced by any pumping well into the production aquifer near the test site, specifically in those locations of the shallow aquifer-aquitard system that remain confined (Carrera and Gaskin, 2007). Therefore, it is recommended to improve the results of the present contribution by accounting for the influence of pumping wells in further analysis.

Acknowledgements

The authors thank Dr. Abdullah Cihan, at Lawrence Berkeley National Laboratory, for provide us with the FORTRAN code ASLMA. We specially thank the two anonymous reviewers for the constructive comments, suggestions and improvements done to the original version of the manuscript.

References

Amelung, F., Galloway, D. L., Bell, J. W., Zebker, H. A. and Laczniak, R. J. (1999). Sensing the ups and downs of Las Vegas: InSAR reveals structural control of land subsidence and aquifer-system deformation. *Geology*, 27(6), pp. 483–486.

Auvinet, G., Méndez, E. and Juárez, M. (2013). Soil fracturing induced by land subsidence in Mexico City, Proceedings of the 18th International Conference on Soil Mechanics and Geotechnical Engineering, Paris, pp. 2921-2924.

Auvinet, G., Méndez, E. and Juárez, M. (2017). El subsuelo de la Ciudad de México, Vol. 3, Supplement to the Third Edition of the book by R.J. Marsal y M. Mazari, Instituto de Ingeniería, UNAM.

Bell, J. W., Amelung, F. Ferretti, A., Bianchi, M. and Novali, F. (2008). Permanent scatterer InSAR reveals seasonal and long-term aquifer-system response to groundwater pumping and artificial recharge, *Water Resources Research*, 44, W02407.

Carrera-Hernández, J. J. and Gaskin, S. J. (2007). The Basin of Mexico aquifer system: regional groundwater level dynamics and database development, *Hydrogeology Journal*, 15, pp. 1577–1590.

Carrera-Hernández, J. J. and Gaskin, S. J. (2009). Water management in the Basin of Mexico: current state and alternative scenarios, *Hydrogeology Journal*, 17, pp. 1483–1494.

Cheng, A. H.-D., and Morohunfola, O. K. (1993). Multilayered leaky aquifer systems: Pumping well solutions, *Water Resources Research*, 29(8), pp. 2787–2800.

Churchill, R. V. (1966). Operational mathematics, 2nd Edition, McGraw-Hill.

Cihan, A., Zhou, Q. and Birkholzer, J. T. (2011a). Analytical solutions for pressure perturbation and fluid leakage through aquitards and wells in multilayered-aquifer systems, *Water Resources Research*, 47, W10504.

Cihan, A., Zhou, Q. and Birkholzer, J. T. (2011b). User Guide for Analytical Solution of Hydraulic Head Changes, Focused and Diffuse Leakage in Multilayered Aquifers (ASLMA), Ernest Orlando Lawrence Berkeley National Laboratory, Earth Sciences Division, pp. 72.

Conagua, (2006). Hacia una estrategia de manejo sustentable de agua en el Valle de México y su zona metropolitana, Gerencia regional XIII, Aguas del Valle de México y Sistema Cutzamala, Comisión Nacional del Agua, México, D.F.

Conagua (2009). Actualización de la disponibilidad media anual de agua subterránea: Acuífero (0901) Zona Zetropolitana de la Cd. de México, Diario oficial de la Federación.

Cruickshank, G. G. (1998). Proyecto Lago de Texcoco: Rescate hidrogeológico, Comisión Federal de Electricidad, CFE, México, D.F.

De Cserna, Z., Aranda-Gómez, J.J., Mitre-Salazar, L.M. (1988). Estructura geológica, gravimetría, sismicidad y relaciones neotectónicas regionales de la cuenca de México: *Boletín del Instituto de Geología*, UNAM, México, 104, 1–71.

DGCOH (1997). Estudio de factibilidad para el reúso de las aguas residuales y pluviales del Valle de México para satisfacer la demanda de agua potable a mediano plazo, a través de la recarga de acuíferos, Instituto de Ingeniería, UNAM.

DGCOH and Lesser (1991). Recarga artificial de agua residual tratada al acuifero del Valle de Mexico, *Ingeniería Hidráulica en México*, pp. 65–70.

Domenico, P. A. and Mifflin, M.D. (1965). Water from low-permeability sediments and land subsidence, *Water Resources Research*, 1(4), pp. 563-576.

Downs, T. J., Mazari-Hiriart, M., Dominguez-Mora, R. and Suffet, I. H. (2000). Sustainability of least cost policies for meeting Mexico City's future water demand, *Water Resources Research*, 36(8), pp. 2321-2339.

Durazo, J. and Farvolden, R. N. (1989). The groundwater regime of the Valley of Mexico from historic evidence and field observations, *Journal of Hydrology*, 112, pp. 171-190.

Enciso-de la Vega, S. (1992). Propuesta de nomenclatura estratigráfica para la cuenca de México, Universidad Nacional Autónoma de México. Instituto de Geología, *Revista*, 10(1), pp. 26–36.

Fries, C. (1960). Geologia del estado de Morelos y de partes adyacente de Mexico y Guerrero, region central meridional de Mexico: Instituto de Geologia, UNAM, Boletin 60, pp. 236.

Gambolati, G., and Teatini, P. (2014). Venice Shall Rise Again—Engineered Uplift of Venice Through Seawater Injection, Elsevier Insights, 100 pp., Elsevier, Amsterdam, Netherlands.

González-Nicolás, A., Baù, D., Cody, B. M., and Alzraiee, A. (2015). Stochastic and global sensitivity analyses of uncertain parameters affecting the safety of geological carbon storage in saline aquifers of the Michigan Basin, *International Journal of Greenhouse Gas Control*, 37, pp. 99-114.

Herrera, I. and Figueroa, G. E. (1969). A correspondence principle for the theory of leaky aquifers, *Water Resources Research*, 5, pp. 900-904.

Herrera, I. (1970). Theory of multiple leaky aquifers, *Water Resources Research*, 6, pp. 185-193.

Herrera, I. (1976). A review of the integrodifferential equations approach to leaky aquifer mechanics, In: Advaces in groundwater hydrology, Ed. Z Saleem, Am. Water Resources Association, pp. 29-47.

Herrera, I., Martínez, R. and Hernández, G. (1989). Contribución para la Administración Científica del Agua Subterránea de la Cuenca de México, *Geofísica Internacional*, 28, pp. 297-334.

Huizar-Álvarez, R., Ouysse, S., Espinoza-Jaramillo, M. M., Carrillo-Rivera, J. J. and Mendoza-Archundia, E. (2016). The effects of water use on Tothian flow systems in the

Mexico City conurbation determined from the geochemical and isotopic characteristics of groundwater, *Environmental Earth Sciences*, 75:1060, pp. 1-17.

Hunt, B. (1985). Flow to a well in a multiaquifer system, *Water Resources Research*, 21, pp. 1637–1641.

Jiménez, C. B., Mazari, H. M., Domínguez, M. R. and Cifuentes, G. E. (2004). El Agua en el Valle de Mexico, In: El agua en Mexico vista desde la academia, Academia Mexicana de Ciencias, Mexico, D.F., pp. 15-32.

Marsal, R. and Mazari, M. (1959). The Subsoil of Mexico City, Contribution to First Pan-American Conf. on Soil Mechanics and Found. Engineering, Facultad de Ingeniería, UNAM, Mexico, 1 and 2.

Mazari, M. and Mackey, D. M. (1993). Potential for groundwater contamination in Mexico City, *Environmental Science and Technology*, 27(5), pp. 794-802.

Mooser, F. (1975). Historia geológica de la Cuenca de México, *In*: Memoria de las obras de drenaje profundo del Distrito Federal, México, D.F., Departamento del Distrito Federal, 38 p.

Mooser, F. and Molia, (1993). Nuevo modelo hidrogeológico para la Ciudad de México, Boletín del Centro de Investigación Sísmica de la Fundación Javier Barros Sierra, 3(1), México.

Neuman, S. P. and Witherspoon, P. A. (1969). Coupled solution for forced recharge in confined aquifers, *Water Resources Research*, 5, pp. 803-816.

NOM-014-CONAGUA-2007. Requisitos para la recarga artificial de acuíferos con agua residual tratada.

NOM-015-CONAGUA-2007. Infiltración artificial de agua a los acuíferos. Características y especificaciones de las obras y del agua.

NRC (1995). Mexico City's water supply: improving the outlook for sustainability. National Academy of Sciences, Washington, DC.

Ortega, G. A. and Farvolden, R. N. (1989). Computer analysis of regional groundwater flow and boundary conditions in the Basin of Mexico, *Journal of Hydrology*, 110, pp. 271-294.

Ortega, G. A., Rudolph, D. L. and Cherry, J. A. (1999). Analysis of long-term land subsidence near Mexico City: Field investigations and predictive modeling, *Water Resources Research*, 35(11), pp. 3327-3341.

Otott, G.E. and Clarke, D.D., (1996). History of the Wilmington field—1986–1996. In: AAPG Pacific Section, Old Oil Fields and New Life: A Visit to the Giants of the Los Angeles Basin, pp. 17–22.

Ovando-Shelley, E., Romo, M. P., Contreras, N. and Giralt, A. (2003). Effects on soil properties of future settlements in downtown Mexico City due to ground water extraction, *Geofísica Internacional*, 42(2), pp. 185-204.

Ovando-Shelley, E., Ossa, A., and Santoyo, E. (2013). Effects of regional subsidence and earthquakes on architectural monuments in Mexico City, *Boletín de la Sociedad Geológica Mexicana*, 65(1), pp. 157-167.

Phien-wej, N., Giao, P.H. and Nutalaya, P. (1998). Field experiment of artificial recharge through a well with reference to land subsidence control, *Engineering Geology*, 50, pp. 187–201.

Poland, J. F. (1972). Subsidence and its control, *In*: Underground Waste Management and Environmental Applications, Cook, T. D. ed., The American Association of Petroleum Geologists, Oklahoma, USA. pp. 50-71.

Poland, J. F. (1984). Guidebook to studies of land subsidence due to groundwater withdrawal, 305 pp., UNESCO, Paris.

Reséndiz, D., Auvinet, G. Méndez, E. (2016). Subsidencia de la Ciudad de México: un proceso centenario insostenible, Instituto de Ingeniería, UNAM, pp. 29.

Rudolph, D. L., Herrera, I. and Yates, R. (1989). Groundwater flow and solute transport in the industrial well fields of the Texcoco saline aquifer system near Mexico City, *Geofísica Internacional*, 28(2), pp. 363–408.

Rudolph, D. L., Cherry, J. A. and Farvolden, R. N. (1991). Groundwater flow and solute transport in fractured lacustrine clay near Mexico City, *Water Resources Research*, 27(9), pp. 2187-2201.

Rudolph, D. L. and Frind, E. O. (1991). Hydraulic response of highly compressible aquitards during Consolidation, *Water Resources Research*, 27(1), pp. 17-30.

Schlaepfer, C. (1968). Hoja Mexico 14Q-h(5), con resumen de la geologia de la hoja Mexico, Distrito Federal y estados de Mexico y Morelos: Instituto de Geologia, UNAM, Carta Geologica de Mexico, Serie de 1:100,000, mapa con texto explicativo en el reverso.

Shi, X., Jiang, S., Xu, H., Jiang, F., He, Z. and Wu, J. (2016). The effects of artificial recharge of groundwater on controlling land subsidence and its influence on groundwater quality and aquifer energy storage in Shanghai, China, *Environmental Earth Sciences*, 75(195), pp. 1-18.

Teatini, P., Ferronato, M., Gambolati, G., Baù, D. and Putti, M. (2010). Anthropogenic Venice uplift by seawater pumping into a heterogeneous aquifer system, *Water Resources Research*, 46, W11547.

Teatini, P., Castelletto, N., Ferronato, M., Gambolati, G. and Tosi, L. (2011). A new hydrogeologic model to predict anthropogenic uplift of Venice, *Water Resources Research*, 47, W12507.

Terzaghi, K. (1925). Principles of soil mechanics, IV—Settlement and consolidation of clay. *Eng. News. Rec.* 95:874–878.

Tolman, C. F. and Poland, J. F. (1940). Groundwater, salt water, infiltration, and ground surface recession in Santa Clara Valley, Santa Clara County, California, American Geophysical Union, pp. 23–34.

Vargas, C. and Ortega, G. A. (2004). Fracture hydraulic conductivity in the Mexico City clayey aquitard: Field piezometer rising-head tests, *Hydrogeology Journal*, 12, pp. 336–344.

Vázquez, S. E. and Jaimes, P. R. (1989). Geología de la Cuenca de México, *Geofísica Internacional*, 28(2), pp. 133–174.

World Bank (2013). Urban Water in the Valley of Mexico: A Green path for Tomorrow. Mexico City, Report 75917, The Word Bank, Washington, USA.

Zhang, Y., Wu, J., Xue, Y., Wang, Z., Yao, Y., Yan, X., and Wang, H. (2015). Land subsidence and uplift due to long-term groundwater extraction and artificial recharge in Shanghai, China, *Hydrogeology Journal*, 23, pp. 1851–1866.

Zhou, Q., Birkholzer, J. T. and Tsang, C. F. (2009). A semi-analytical solution for large-scale injection-induced pressure perturbation and leakage in a laterally bounded aquifer-aquitard system, *Transport in Porous Media*, 78(1), pp. 127–148.

Zhou, X. and Burbey, T. J. (2014). Deformation characteristics of a clayey interbed during fluid injection, *Engineering Geology*, 183, pp. 185–192.

Zeevaert, L. (1982). Foundation Engineering for Difficult Subsoil Conditions, 2nd ed., Van Nostrand-Reynhold Company, New York, NY, USA.